

A Dual-Burst Geometrical Prescription for Concurrent Signaling

NAOKI SETO¹

¹*Department of Physics, Kyoto University, Kyoto 606-8502, Japan*

ABSTRACT

We propose a dual-burst implementation of concurrent signaling for technosignature searches. Concurrent signaling is a Schelling-point prescription for implicit coordination between transmitters and receivers without prior communication, using salient astronomical phenomena as coordination anchors. It allows possible transmitters at different line-of-sight distances to be searched collectively through a time-dependent locus on the sky. In the dual-burst implementation, the coordination anchors are two cosmological transients. At a chosen observing time after the later burst, the leading geometrical prescription specifies a precisely defined sky ring from the two burst directions and their observed arrival times at the receiver. No distance to either burst, to a candidate transmitter, or to a Galactic spatial anchor is required to construct this angular search locus. The finite width of the ring is therefore controlled primarily by burst localization rather than by an astrophysical distance scale, thereby reducing the set of sky directions to be searched.

Keywords: extraterrestrial intelligence, astrobiology, gamma-ray bursts, methods: analytical

1. INTRODUCTION

A central difficulty in searches for intentional interstellar signals is the size of the signaling parameter space. A receiver must choose not only where to look on the sky, but also when to look, over what frequency or wavelength range, and for what class of signal morphology (e.g., Tarter 2001; Horowitz & Sagan 1993; Wright 2020). The transmitter faces a related problem: without prior coordination, it is inefficient to transmit arbitrarily over the full space of directions, times, and signal types. An efficient strategy should therefore exploit references and rules that both sides can identify independently.

This is the role of a Schelling point. In the present context, a Schelling point is not merely a conspicuous object, but a basis for implicit coordination in a shared strategy space (Schelling 1960). Useful prescriptions should therefore be simple and reproducible, preferably tied to salient astronomical events or symmetric geometrical structures rather than to arbitrary private choices. Such a prescription can guide both when transmitters send and when receivers search.

Concurrent signaling is one way to implement this idea (Seto 2019, 2021, 2024), and is closely related to earlier timing-based SETI strategies that use conspicuous astronomical events. In early SETI Ellipsoid work, a single transient

event and the distance to a target star define a predicted reception epoch for a signal timed to that event, making accurate target distances an essential part of the prescription (McLaughlin 1977; Makovetskii 1980; Lemarchand 1994) (see also Davenport et al. 2022; Nilipour et al. 2023; Cabrales et al. 2024 for recent observational studies). By contrast, in a concurrent-signaling scheme, a given sky direction is searched at a specified observing epoch. The search then covers possible transmitters in that direction over a range of line-of-sight distances, rather than being tied to a single target distance. This is achieved by assigning, for each possible signal trajectory, a common reference point and a common reference time that can be determined independently by transmitters and receivers. The transmitter-side and receiver-side tasks are then two sides of the same prescription: a transmitter decides whether and when to emit relative to its assigned reference event, while the receiver applies the same rule to decide where and when to search. The key problem is therefore how to define these common reference points and times using astronomical information available to both sides.

Earlier implementations realized this assignment by using a finite-distance astronomical reference. In schemes based on a single finite-distance anchor, the reference event itself had to provide both a well-defined epoch and a three-dimensional position. A later hybrid strategy reduced this burden by using an extragalactic burst as a temporal marker and the Galactic center as a spatial reference (Seto 2025). However, any prescription tied to a finite-distance spatial anchor retains a

distance-error term and a corresponding reference-selection ambiguity. A prescription based only on timing and direction would have a cleaner error hierarchy and would be a natural target for implicit coordination among independently acting participants.

The present paper removes the finite-distance spatial reference by using two distant bursts. A single distant burst provides a salient time marker and sky direction for each observer, but it does not by itself define spacetime reference events for signal trajectories across the Galaxy. Two distant bursts provide the minimal additional structure: the local encounters of their wavefronts define such reference events across the Galaxy, as illustrated in Figure 1. We use these encounters as virtual-emission events, to which outgoing virtual rays with their associated emission times are assigned. A transmitter may emit an artificial signal along one of these assigned virtual rays, while a receiver applies the same prescription to determine the corresponding arrival directions at a chosen observing time. The construction is geometrical rather than tied to a particular coordinate frame; a receiver frame is introduced below only to compute the resulting search ring.

In the plane-wave approximation, the receiver-side search directions, and hence the predicted sky ring, depend only on the two burst directions and their observed arrival times. No distance to either burst, to a candidate transmitter, or to a Galactic spatial anchor is required. The predicted search ring is therefore controlled primarily by the angular localizations of the two bursts rather than by an astrophysical distance scale. Although we use gamma-ray bursts (GRBs) as the main working example, the same construction applies to any pair of sufficiently distant, conspicuous, and well-localized transients with well-defined arrival times (see also Corbet 1999).

In this paper we develop the geometry of this dual-burst prescription. We first formulate the virtual-emission rule and derive the exact plane-wave search ring for an arbitrary observing time after the later burst. We then examine the ring geometry, its small-angle form, and the associated virtual-emission depth scale. After estimating the leading error budget, we discuss burst-pair selection as the remaining Schelling-like problem. We do not perform a survey-data analysis here; the goal is to provide a compact geometrical prescription that can be applied to archival or future time-domain SETI searches.

2. DUAL-BURST PRESCRIPTION AND SEARCH RING

We now turn the dual-burst idea into an explicit search prescription for a receiver at the Solar System. As illustrated in Figure 1, the local encounters of the two burst wavefronts define virtual reference events across the Galaxy. To each event we assign outgoing virtual rays, understood as lightlike

trajectories with their corresponding virtual-emission times. A transmitter located on one such ray may emit an artificial signal along the assigned virtual ray, while a receiver applies the same prescription to determine which arrival directions should be searched at a chosen observing time. We now derive the corresponding search ring.

Consider two distant bursts, A and B, observed at the Solar System at times t_A and t_B , respectively, with $t_B > t_A$. Let $\Delta \equiv t_B - t_A > 0$, and let $\hat{\mathbf{b}}_A$ and $\hat{\mathbf{b}}_B$ be the corresponding source directions on the sky, pointing from the Solar System toward the two bursts. We denote their angular separation by $\cos \alpha = \hat{\mathbf{b}}_A \cdot \hat{\mathbf{b}}_B$. For an observing time $T = t_B + \tau$, define the dimensionless delay $u = \tau / \Delta$.

We work in a Solar-System-barycentric inertial frame, with the Solar System at $\mathbf{x} = 0$ and coordinate time t . In the plane-wave approximation, the wavefronts of bursts A and B are represented by

$$t - t_A + \frac{\hat{\mathbf{b}}_A \cdot \mathbf{x}}{c} = 0, \quad t - t_B + \frac{\hat{\mathbf{b}}_B \cdot \mathbf{x}}{c} = 0. \quad (2.1)$$

Now consider a virtual ray whose corresponding signal is received at the Solar System at

$$T = t_B + \tau, \quad \tau > 0. \quad (2.2)$$

If it arrives from sky direction $\hat{\mathbf{n}}$, with $\hat{\mathbf{n}}$ a unit vector pointing from the Solar System along the arrival direction, and the associated virtual-emission event is at distance s along that direction, then the event is

$$(t, \mathbf{x}) = \left(t_B + \tau - \frac{s}{c}, s\hat{\mathbf{n}} \right). \quad (2.3)$$

The dual-burst prescription requires this event to lie on both burst wavefronts. Substituting Eq. (2.3) into Eq. (2.1) gives

$$\Delta + \tau = \frac{s}{c} \left(1 - \hat{\mathbf{b}}_A \cdot \hat{\mathbf{n}} \right), \quad \tau = \frac{s}{c} \left(1 - \hat{\mathbf{b}}_B \cdot \hat{\mathbf{n}} \right). \quad (2.4)$$

Eliminating s , we obtain the plane-wave search-ring equation

$$\left[(1+u)\hat{\mathbf{b}}_B - u\hat{\mathbf{b}}_A \right] \cdot \hat{\mathbf{n}} = 1. \quad (2.5)$$

At a fixed observing time $T = t_B + \tau$, this equation restricts the unit arrival direction $\hat{\mathbf{n}}$ to the intersection of the unit sphere with a plane. As shown explicitly in the next section, this locus is a small circle, or search ring.

Equation (2.5) is the central plane-wave result of the construction. The predicted search ring depends only on the burst directions $\hat{\mathbf{b}}_A$, $\hat{\mathbf{b}}_B$, the observed arrival-time separation Δ , and the elapsed observing time τ . It does not require the distances to the bursts, the distance to a possible transmitter, or the distance to any Galactic spatial anchor. This distance independence follows from treating the distant-burst wavefronts as plane waves; for cosmological bursts, we show

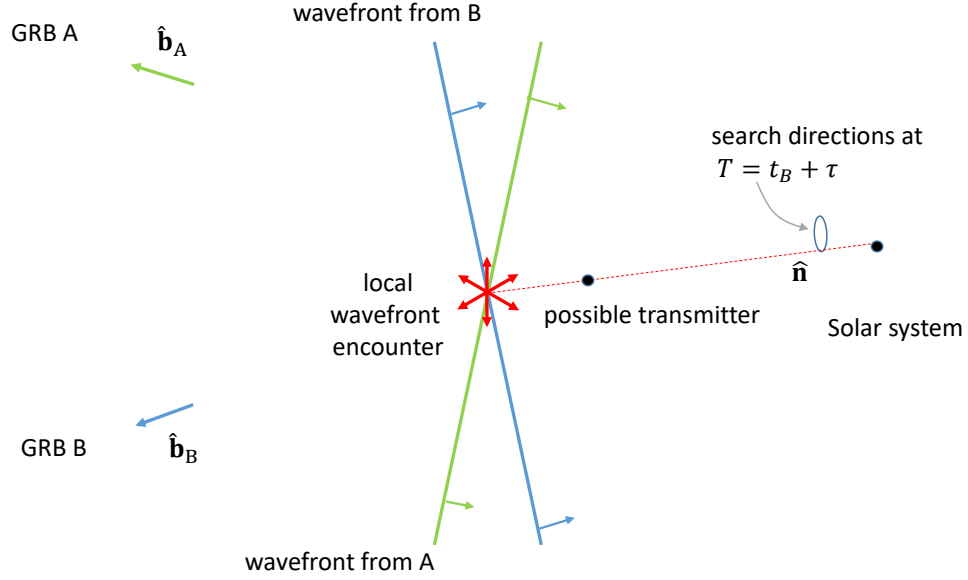


Figure 1. Schematic illustration of the dual-burst virtual-emission prescription. Two distant bursts, A and B, are observed by the receiver, here taken to be the Solar System, at times t_A and t_B , and are represented by approximately planar wavefronts associated with the unit source directions $\hat{\mathbf{b}}_A$ and $\hat{\mathbf{b}}_B$. Each local encounter of the two wavefronts defines a reference event of the prescription. The encounter shown here is only a representative example; in three-dimensional space, the set of such encounters forms a two-dimensional surface. Isotropic outgoing virtual rays are assigned to these reference events. A possible transmitter located on one such ray may emit an artificial signal along that virtual ray. For an observing time $T = t_B + \tau$, a receiver applies the same prescription to determine the corresponding arrival directions $\hat{\mathbf{n}}$ on the sky, forming the search ring derived in Section 2. In the plane-wave approximation, this construction depends only on the two burst directions and their observed arrival times, not on the distances to the bursts, to the transmitter, or to any Galactic spatial anchor.

below that the corresponding curvature correction is smaller than the angular localization scale relevant for the searches considered here.

The same equations also give the line-of-sight distance to the corresponding virtual-emission event. From the second of Eqs. (2.4),

$$s(\hat{\mathbf{n}}, \tau) = \frac{c\tau}{1 - \hat{\mathbf{b}}_B \cdot \hat{\mathbf{n}}}. \quad (2.6)$$

Thus the search direction $\hat{\mathbf{n}}$ and the associated virtual-emission depth s are both determined by timing and angular information alone.

Equation (2.6) is written for the Solar System endpoint, but it reflects a more general causal ordering along the assigned virtual ray. At any point on that ray, the time interval between the local arrival of the later burst B and the arrival of the virtual photon is proportional to the path length from the corresponding local wavefront encounter to that point. This interval is therefore non-negative, and vanishes only at the encounter itself. A transmitter on the ray can therefore emit after receiving both burst wavefronts at its own location, rather than anticipating the later burst.

3. SEARCH-RING GEOMETRY AND DEPTH SCALE

We now examine the geometry of Eq. (2.5) for $u \geq 0$. It is useful to define

$$\mathbf{q}(u) \equiv (1+u)\hat{\mathbf{b}}_B - u\hat{\mathbf{b}}_A. \quad (3.7)$$

Then the exact search condition is

$$\mathbf{q}(u) \cdot \hat{\mathbf{n}} = 1. \quad (3.8)$$

This is the intersection of the unit sphere with a plane, and therefore defines a small circle on the sky. Its center direction is the direction of $\mathbf{q}(u)$, and its angular radius ρ is determined by

$$\cos \rho(u) = \frac{1}{|\mathbf{q}(u)|}. \quad (3.9)$$

Using $\cos \alpha = \hat{\mathbf{b}}_A \cdot \hat{\mathbf{b}}_B$, we obtain

$$|\mathbf{q}(u)|^2 = 1 + 2u(1+u)(1 - \cos \alpha) \geq 1. \quad (3.10)$$

At $u = 0$, Eq. (3.7) gives $\mathbf{q} = \hat{\mathbf{b}}_B$, so the ring is collapsed in the direction of burst B. As u increases, the term $-u\hat{\mathbf{b}}_A$ shifts the center direction $\mathbf{q}(u)$ from B toward the side opposite to A on the sky. For any nonzero burst separation, Eq. (3.10) shows that $|\mathbf{q}(u)|$ increases monotonically with u . Since $\cos \rho = 1/|\mathbf{q}|$, the angular radius also grows monotonically with observing time.

In the small-angle limit $\alpha \ll 1$, this motion has a particularly simple form. Project the sky near burst B onto a tangent plane, and place burst A at angular displacement \mathbf{a} from B, with $|\mathbf{a}| = \alpha$. Then the ring center is displaced from B by $-u\mathbf{a}$, while the ring radius is

$$\rho_{\text{ring}} = \alpha \sqrt{u(1+u)}. \quad (3.11)$$

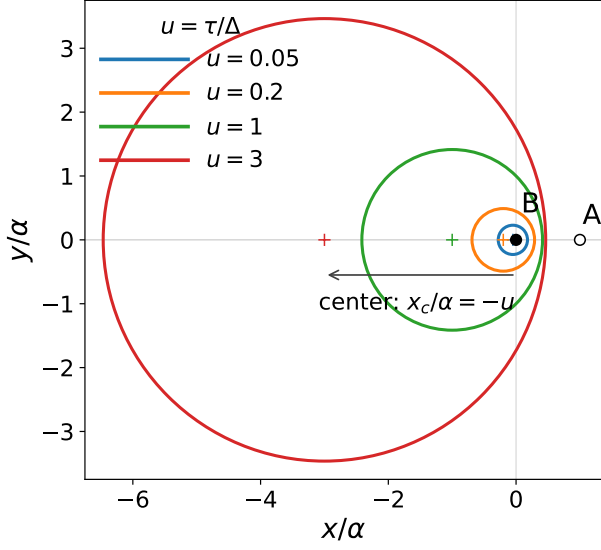


Figure 2. Small-angle illustration of the search-ring evolution in the tangent plane centered on burst B. Coordinates are measured in units of the burst separation α , with B at the origin and A at $x/\alpha = 1$. At dimensionless observing delay $u = \tau/\Delta$, the ring center is displaced to $x/\alpha = -u$, while the ring radius is $\rho_{\text{ring}}/\alpha = \sqrt{u(1+u)}$. Thus the ring center moves from B toward the side opposite to A, while the ring radius grows with time.

Thus, in units of the burst separation, the center displacement is u , and the radius is $\sqrt{u(1+u)}$. This is the geometry illustrated in Figure 2.

The associated line-of-sight depth is given by Eq. (2.6). At a fixed observing time, the sky directions $\hat{\mathbf{n}}$ are restricted to the search ring, but the quantity $\hat{\mathbf{b}}_B \cdot \hat{\mathbf{n}}$ is not constant around that ring. The virtual-emission depth is therefore not uniform along the ring. Points on the side of the ring toward burst A have larger $\hat{\mathbf{b}}_B \cdot \hat{\mathbf{n}}$, and hence correspond to larger depths, whereas points on the opposite side are shallower. The depth distribution for any chosen pair and observing time can be computed directly from Eq. (2.6).

For pair selection, it is useful to introduce a characteristic depth scale by evaluating the denominator at the burst separation angle:

$$s_B \equiv \frac{c\Delta}{1 - \cos\alpha} \simeq \frac{2c\Delta}{\alpha^2}. \quad (3.12)$$

Numerically,

$$s_B \simeq 20.1 \text{ kpc} \left(\frac{\Delta}{10 \text{ yr}} \right) \left(\frac{\alpha}{1^\circ} \right)^{-2}. \quad (3.13)$$

Thus decade-separated burst pairs with angular separations of order one degree naturally probe Galactic-scale distances.

The scale in Eq. (3.13) is not merely formal. Existing GRB records include pairs satisfying these criteria. As an illustrative check, Table 1 lists examples with $0.9^\circ \leq \alpha \leq 1.1^\circ$, $\Delta \geq 10 \text{ yr}$, and $\sigma_A, \sigma_B \leq 1''$, where σ_A and σ_B denote the adopted

Table 1. Illustrative GRB pairs near $\alpha \simeq 1^\circ$. The pairs satisfy $0.9^\circ \leq \alpha \leq 1.1^\circ$, $\Delta \geq 10 \text{ yr}$, and $\sigma_A, \sigma_B \leq 1''$ in the working catalog used here. The column b_B gives the Galactic latitude of the later burst, which approximates the early sky region sampled by the ring.

Pair	Δt (yr)	α (deg)	s_B (kpc)	b_B (deg)	σ_A, σ_B (arcsec)
061222B–251103B	18.87	1.094	31.7	−8.6	0.79, 0.93
081102A–230409B	14.43	1.013	28.3	−1.6	0.70, 0.93
060512A–190211A	12.75	1.021	24.6	+74.8	0.23, 0.25
081121A–200630A	11.60	1.017	22.6	−29.0	0.28, 0.93
090726A–200829A	11.09	0.937	25.5	+35.2	0.70, 0.16

angular localization uncertainties of the two bursts. The examples are selected from a working catalog constructed from the public GRBWeb database.

4. ERROR BUDGET

For an observational use of the prescription, one chooses an ordered burst pair (A, B) with $t_B > t_A$, adopts the observed burst directions $\hat{\mathbf{b}}_A, \hat{\mathbf{b}}_B$, and computes the receiver-frame arrival-time separation $\Delta = t_B - t_A$. For a chosen observing epoch $T = t_B + \tau$, the delay τ fixes the dimensionless time $u = \tau/\Delta$. Substituting these quantities into Eq. (2.5) gives the corresponding angular search ring. Timing errors in the burst arrival times affect the ring only through u , and are typically much smaller than the angular-localization errors considered here. The dominant geometrical uncertainty is therefore expected to come from the angular localizations of the two bursts.

The small-angle form of Section 3 makes the error scaling transparent. The burst-position errors affect the search ring in two geometrically distinct ways: they shift the ring center on the sky and they change the ring radius. Keeping only the leading terms in the tangent-plane approximation, the center uncertainty is

$$\sigma_c^2(u) \simeq (1+u)^2 \sigma_B^2 + u^2 \sigma_A^2. \quad (4.14)$$

The corresponding radial uncertainty is

$$\sigma_\rho^2(u) \simeq u(1+u)\sigma_\alpha^2, \quad \sigma_\alpha^2 \simeq \sigma_A^2 + \sigma_B^2, \quad (4.15)$$

where σ_A and σ_B are the characteristic angular localization errors of the two bursts, and σ_α denotes the uncertainty in their angular separation, approximated here by adding the independent projected errors in quadrature. Thus, for comparable burst localizations, the characteristic width of the search ring is of order $(1+u)\sigma_\alpha$, up to factors of order unity. The key point is that the width is controlled by burst localization, not by any astrophysical distance uncertainty.

It is useful to compare this scale with the finite-anchor hybrid construction of Seto (2026). In the GRB–TESS application discussed there, the search ring has a radius of order $\rho \simeq$

0.8° , and its width is mainly controlled by the fractional uncertainty in the Galactic-center distance. With $\delta D_{\text{GC}}/D_{\text{GC}} \simeq 5 \times 10^{-3}$ (GRAVITY Collaboration et al. 2021), this gives an anchor-induced angular width of order

$$\frac{1}{2}\rho \frac{\delta D_{\text{GC}}}{D_{\text{GC}}} \sim 10''. \quad (4.16)$$

By contrast, in the present dual-burst construction, the corresponding width is set by the burst localizations. For well-localized pairs with subarcsecond burst positions and $u = O(1)$, the characteristic width can therefore be substantially narrower.

The plane-wave approximation introduces one additional systematic check. For a burst at finite distance R , the incoming wavefront is spherical rather than exactly planar. Expanding the corrected arrival-time function for $s \ll R$, where s is the virtual-emission distance, gives a characteristic angular displacement of order

$$\delta\theta_{\text{curv}} \sim \frac{s\theta}{2R} \simeq 0.36 \text{ arcsec} \left(\frac{s}{20 \text{ kpc}} \right) \left(\frac{\theta}{1^\circ} \right) \left(\frac{R}{100 \text{ Mpc}} \right)^{-1}, \quad (4.17)$$

where θ is the angular offset from the burst direction. For typical cosmological GRBs, R is much larger than 100 Mpc, so the plane-wave approximation has a large margin. Even at $R \sim 100$ Mpc, the curvature-induced displacement in Eq. (4.17) remains below the arcsecond scale for the Galactic-scale depths and degree-scale angular offsets considered here. When the distance to a reference burst is known, the same calculation can be repeated with the corresponding spherical wavefront if a narrower search mask requires it. This provides a controlled finite-distance extension of the plane-wave approximation.

5. SEARCH STRATEGIES

The dual-burst prescription removes the need for a finite-distance spatial anchor, but it leaves a new Schelling-like problem: the selection of the burst pair itself. If a catalog contains N usable bursts, there are $N(N-1)/2$ possible pairs, so an arbitrary pair choice is not a plausible basis for implicit coordination. A useful strategy must therefore reduce this pair space by a rule that is simple, reproducible, and based on information available in common burst records.

We focus on two such reductions: anchoring the pair to an exceptionally salient burst, and selecting pairs whose geometry is favorable for Galactic searches.

5.1. Salient-burst anchored pairs

The most direct way to reduce the burst-pair selection problem is to require one or both members of the pair to be exceptionally salient. This converts an unrestricted choice among many possible pairs into a smaller set anchored by conspicuous events. Such anchors are attractive as Schelling

references because they can be selected independently from commonly available burst records.

GRB 221009A provides the clearest current example. Its observed fluence was far above that of other well-documented GRBs (Burns et al. 2023; Frederiks et al. 2023; Lesage et al. 2023), motivating its description as the “brightest of all time” (BOAT) GRB (Burns et al. 2023). This exceptional brightness corresponds to an inferred rarity of order one event per 10^4 yr, making it a particularly natural Schelling anchor (Seto 2025). Its low Galactic latitude, $b \simeq 4.3^\circ$, further makes it attractive for searches involving dense Galactic stellar fields.

5.2. Geometrically favorable pair selection

The geometrical role of pair selection is to tune the search ring to the Galactic stellar distribution. The key parameters are the angular separation α and the time separation Δ . As shown in Section 3, these control the characteristic virtual-emission depth,

$$s_B \simeq \frac{2c\Delta}{\alpha^2} \simeq 20.1 \text{ kpc} \left(\frac{\Delta}{10 \text{ yr}} \right) \left(\frac{\alpha}{1^\circ} \right)^{-2}, \quad (5.18)$$

and, at fixed $u = \tau/\Delta$, the angular size of the ring,

$$\rho_{\text{ring}} = \alpha \sqrt{\frac{\tau}{\Delta} \left(1 + \frac{\tau}{\Delta} \right)}. \quad (5.19)$$

Thus smaller angular separations give deeper and narrower rings, whereas larger angular separations give shallower and wider rings. The time separation Δ sets the overall depth scale and determines how a given observing delay maps to u .

The favorable choice of α and Δ is therefore not universal. Toward the Galactic disk, increasing the characteristic depth can sample dense stellar regions over a longer path length. At high Galactic latitude, by contrast, the line of sight quickly leaves the thin disk, so increasing s_B does not necessarily add many Galactic targets. In such directions, angular coverage and ring motion can be more important than depth alone. A practical pair ranking should therefore combine the geometric scalings above with the Galactic stellar distribution and the available time-domain survey coverage.

A complementary use of the same pair-selection framework is to start from a specific line of sight rather than from a sky ring. For example, one may ask whether a ring generated by a focal burst pair crosses the direction of a known astrobologically interesting stellar target, and at what observing epoch this occurs. This target-specific version still uses only the stellar direction, not the stellar distance, and therefore retains the distance-free character of the prescription. Such applications form a natural search-design extension of the present geometrical prescription, connecting it to targeted optical or radio SETI searches where particular stellar directions and observing windows must be prioritized.

6. SUMMARY AND DISCUSSION

We proposed a dual-burst SETI prescription in which two distant astrophysical transients provide a distance-free reference structure for concurrent signaling. The local encounters of the two burst wavefronts define reference events, and outgoing virtual rays from those events define the corresponding signal trajectories. In the plane-wave approximation, the resulting search ring, Eq. (2.5), depends only on the two burst directions, their observed arrival-time separation, and the chosen observing time, not on the distances to the bursts, to a possible transmitter, or to any Galactic spatial anchor.

We derived the ring geometry, the associated virtual-emission depth, and the leading error budget. The characteristic depth scale $s_B \simeq 2c\Delta/\alpha^2$ shows that decade-separated GRB pairs with degree-scale angular separations naturally probe Galactic-scale distances. For suitably well-localized pairs, the leading ring width is set by burst localization

rather than by any astrophysical distance uncertainty, allowing arcsecond-scale search rings in favorable cases.

The removal of a finite-distance spatial anchor shifts the remaining Schelling problem to burst-pair selection. We emphasized that the pair should be chosen using simple and reproducible criteria, such as the salience of an exceptionally bright burst, the angular and temporal separations of the pair, localization quality, and the Galactic stellar distribution sampled by the resulting ring. GRB 221009A provides a natural example of a salient anchor, while existing GRB records include decade-separated pairs satisfying the illustrative Galactic-depth criteria discussed above.

The formulae above are intended as the leading geometrical prescription. When constructing search masks substantially narrower than an arcsecond, one can use the usual high-precision astrometric and time-standard procedures, including relativistic corrections where needed.

1 The author thanks Y. Uno for useful conversations.

REFERENCES

- Burns, E., Svinkin, D., Fenimore, E., et al. 2023, *ApJL*, 946, L31, doi: [10.3847/2041-8213/acc39c](https://doi.org/10.3847/2041-8213/acc39c)
- Cabrales, B., Davenport, J. R. A., Sheikh, S., & et al. 2024, *AJ*, 167, 101, doi: ...
- Corbet, R. H. D. 1999, *Publ. Astron. Soc. Pac.*, 111, 881, doi: [10.1086/316395](https://doi.org/10.1086/316395)
- Davenport, J. R. A., Cabrales, B., Sheikh, S., & et al. 2022, *AJ*, 164, 117, doi: ...
- Frederiks, D., Svinkin, D., Lysenko, A. L., et al. 2023, *ApJL*, 949, L7, doi: [10.3847/2041-8213/acd1eb](https://doi.org/10.3847/2041-8213/acd1eb)
- GRAVITY Collaboration, Abuter, R., Amorim, A., et al. 2021, *A&A*, 647, A59, doi: [10.1051/0004-6361/202040208](https://doi.org/10.1051/0004-6361/202040208)
- Horowitz, P., & Sagan, C. 1993, *The Astrophysical Journal*, 415, 218, doi: [10.1086/173164](https://doi.org/10.1086/173164)
- Lemarchand, G. A. 1994, *Ap&SS*, 214, 209, doi: [10.1007/BF00982337](https://doi.org/10.1007/BF00982337)
- Lesage, S., Veres, P., Briggs, M. S., et al. 2023, *ApJL*, 952, L42, doi: [10.3847/2041-8213/ace5b4](https://doi.org/10.3847/2041-8213/ace5b4)
- Makovetskii, P. V. 1980, *Icarus*, 41, 178, doi: [10.1016/0019-1035\(80\)90002-0](https://doi.org/10.1016/0019-1035(80)90002-0)
- McLaughlin, W. I. 1977, *Icarus*, 32, 464, doi: [10.1016/0019-1035\(77\)90019-7](https://doi.org/10.1016/0019-1035(77)90019-7)
- Nilipour, A., Davenport, J. R. A., Croft, S., & Siemion, A. P. V. 2023, *AJ*, 166, 79, doi: [10.3847/1538-3881/acde79](https://doi.org/10.3847/1538-3881/acde79)
- Schelling, T. C. 1960, *The Strategy of Conflict* (Harvard University Press)
- Seto, N. 2019, *The Astrophysical Journal Letters*, 876, L10, doi: [10.3847/2041-8213/ab133a](https://doi.org/10.3847/2041-8213/ab133a)
- . 2021, *The Astrophysical Journal*, 917, 96, doi: [10.3847/1538-4357/ac0c7b](https://doi.org/10.3847/1538-4357/ac0c7b)
- . 2024, *The Astrophysical Journal*, 964, 105, doi: [10.3847/1538-4357/ad2a48](https://doi.org/10.3847/1538-4357/ad2a48)
- . 2025, *Astrophys. J.*, 994, 135, doi: [10.3847/1538-4357/ae06a8](https://doi.org/10.3847/1538-4357/ae06a8)
- Seto, N. 2026, *ApJ*, 1001, 117, doi: [10.3847/1538-4357/ae48ea](https://doi.org/10.3847/1538-4357/ae48ea)
- Tarter, J. C. 2001, *Annual Review of Astronomy and Astrophysics*, 39, 511, doi: [10.1146/annurev.astro.39.1.511](https://doi.org/10.1146/annurev.astro.39.1.511)
- Wright, J. T. 2020, *International Journal of Astrobiology*, 19, 446, doi: [10.1017/S1473550420000221](https://doi.org/10.1017/S1473550420000221)